



A Heteroclinic Bifurcation in a Motion of Pendulum: Numerical-Topological Approach

Ibrahim Jawarneh¹ · Zuhier Altawallbeh²

Accepted: 9 March 2022 / Published online: 16 April 2022

© The Author(s), under exclusive licence to Springer Nature India Private Limited 2022

Abstract

Dynamical systems are frequently modeled by differential equations, the change in the solution structure of such systems as parameters vary is fundamental for understanding the phenomena. In this paper, we consider a system of differential equations with a parameter γ , which is understood from mechanics of a pendulum moving in the potential energy $V_\gamma(x) = \frac{x^2}{2} - \gamma \frac{x^3}{3} - \frac{x^4}{4}$, $\gamma > 0$. The global dynamics and the steady state of the system are analyzed. We verify and prove the existence of the heteroclinic bifurcation between two saddles of the system using numerical and topological methods.

Keywords Pendulum · Heteroclinic orbit · Stability analysis · Applied algebraic topology · Morse set · Conley index

Mathematics Subject Classification 37B30 · 37C29 · 34C23 · 70F40 · 74H15

Introduction

Dynamical systems usually represent classical mechanics using differential equations. The control theory deals with influencing the behavior of these dynamics. Recently, many studies have been conducted to explain exciting models, see [1, 2, 8, 12, 16, 17, 19, 20]. A pendulum is a motivating example, which has been studied for many centuries. The first study of the pendulum was started by Italian scientist Galileo Galilei after he watched a suspended lamp swing back and forth in 1588, he began serious investigations in 1602. Later on, French physicist Jean Foucault developed the Foucault pendulum. He used it in 1851 to show the earth's rotation, see [4]. In 1953, Hughes studied the properties of the simple pendulum, see [15].

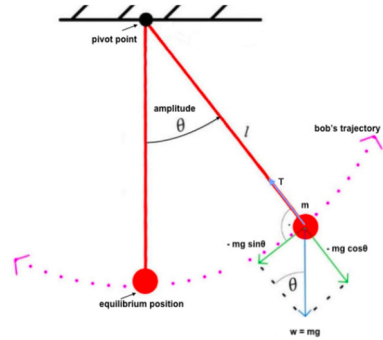
✉ Ibrahim Jawarneh
ibrahim.a.jawarneh@ahu.edu.jo

Zuhier Altawallbeh
Zuhier1980@gmail.com

¹ Department of Mathematics, Al-Hussein Bin Talal University, Ma'an 71111, Jordan

² Department of Mathematics, Tafila Technical University, Tafila 66110, Jordan

Fig. 1 A pendulum in motion



The pendulum system has many interesting bifurcations, see [3, 13, 22, 26, 28, 30]. In particular, we can find the heteroclinic bifurcation in many studies that have been conducted to understand the pendulum system. Dabbs and Smith in [6] used planar Melnikov techniques to determine a parameter set that preserves the coexistence of both heteroclinic and homoclinic orbits in a rotating pendulum. In [7], the nonlinear oscillations of the forced and damped rotating pendulum was explored, and the Melnikov functions due to the heteroclinic orbit was computed to reveal the transverse heteroclinic orbit. The splitting of heteroclinic orbits was accomplished in [18] by discretizing spatial or temporal derivatives in nonlinear equations that supported such solutions. According to Rabinowitz [24], there are heteroclinic orbits of autonomous Hamiltonian systems connecting two equilibria. In [29], a specific case of autonomous Hamiltonian systems was considered, and analytic methods were utilized to establish the existence of the heteroclinic orbits of discrete pendulum equation linking every two adjacent points.

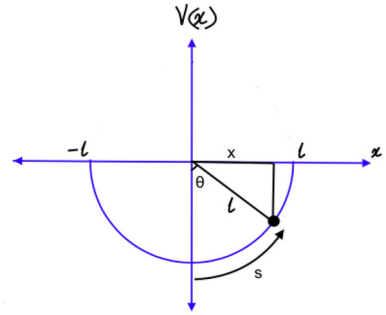
In this research, we explain the construction of a motion of pendulum system in potential energy that is found in [14]. We use the combination of the numerical method and topological theorems that has been successfully applied to the existence of bifurcation in dynamical systems. In particular, we study the stability of the desired system, and we use the Maple software to show the phase portrait of before, after and at heteroclinic bifurcation where the value of the parameter γ is approximated. Then, the Conley index theorems and Morse sets are applied to prove the existence of the heteroclinic bifurcation in the system. To make a conceptual idea of a motion of pendulum with potential energy $V(x)$, we should understand the similarity between the bead-on-wire and the pendulum. Take a pendulum whose motion is restricted to a plane (moves in one direction), with a bob (mass m) on a string of length l , as illustrated in Fig. 1. The arc length of the pendulum is $l\theta$ (theta in radians), the velocity of the bob is $l\theta'$, and the tangential component of its acceleration is $l\theta''$. The forces acting on the bob of a pendulum are its weight $w = mg$ (g is gravity) and the tension T of the string. Newton's second law is one of the most important in all of physics, the vector sum of the forces F acting on an object is equal to the object's mass m multiplied by its acceleration a as in the Eq. (1).

$$F = ma. \tag{1}$$

Using Fig. 1 and the fact $a = l\theta''$, the Eq. (1) can be written in terms of θ to depict the action of the pendulum as moving opposite to

$$-mg \sin(\theta) = ml\theta''. \tag{2}$$

Fig. 2 Bead on a wire of semi circular shape



which is equivalent to

$$\theta'' = -K \sin(\theta), \left(\frac{g}{l}\right) = K. \tag{3}$$

The Eq. (3) is second order differential equation that shows the motion of the pendulum with one variable θ . In order to solve the Eq. (3), we rewrite it in first order by putting $y = \theta'$ then $y' = \theta''$, so we get the following system of first order of differential equations

$$\begin{aligned} \theta' &= y, \\ y' &= -K \sin(\theta). \end{aligned} \tag{4}$$

On the other hand, a physical particle moving without friction in a style involving only one variable x , the potential energy $V(x)$ is introduced by a general theory in physics, which is defined by the force equation

$$mx'' = -\frac{dV(x)}{dx}. \tag{5}$$

The one parameter mechanical system (5) is second order differential equation that can be converted to system of first order differential equations by putting $y = mx'$ then $y' = mx''$ to get the following system

$$\begin{aligned} x' &= m^{-1}y, \\ y' &= -\frac{dV(x)}{dx}. \end{aligned} \tag{6}$$

where y represents the velocity of the particle up to a constant multiple. The solution of Eq. (5) acts almost like the x -coordinate of a bead of mass m sliding without friction on a wire whose graph is $V(x)$ in a constant gravitational field with $g = 1$. The equation $F = ma$ describes the motion of the bead with acceleration in terms of the arc length. To go over the details, let s be the arc length along the wire of a semi circular shape as shown in Fig. 2 (If $s(t)$ describes the motion of the bead, $s''(t)$ is the acceleration), then $V(x) = -\sqrt{l^2 - x^2}$. As $x = l \sin(\theta)$, we have

$$\frac{dV}{dx} = \frac{x}{\sqrt{l^2 - x^2}} = \frac{l \sin \theta}{l \cos \theta} = \tan \theta \tag{7}$$

Because the arc length along the wire is measured by $s(x)$.

$$s(x) = \int_0^x \sqrt{1 + (dV/dx)^2} \tag{8}$$

Then

$$\frac{dV}{ds} = \frac{dV/dx}{ds/dx} = \frac{dV/dx}{\sqrt{1 + (dV/dx)^2}} \tag{9}$$

Using the fact $s''(t) = -\frac{dV}{ds}$, the force can be written as in the following

$$F = ms''(t) = -m \frac{dV}{ds} = -m \frac{dV/dx}{\sqrt{1 + (dV/dx)^2}} = -m \frac{\tan \theta}{\sqrt{1 + \tan^2 \theta}} = -m \sin \theta \quad (10)$$

This implies the Eq. (11) that describes the motion of a bead on a circular wire.

$$s'' = -\sin \theta \quad (11)$$

As $s = l\theta$, the Eq. (11) can be written as

$$\theta'' = -(1/l) \sin \theta \quad (12)$$

which describes the motion of pendulum in Eq. (3). Thus, the analogy between the pendulum and the bead-on-wire is completed.

Back to the pendulum system, Eqs. (3) and (4) are of the proper mathematical form (5) and (6) for a mechanical system with one degree of freedom, so there exists a potential function $V(\theta)$. Combining Eqs. (3) and (5) implies that

$$\frac{dV(\theta)}{d\theta} = K \sin(\theta) \quad (13)$$

Adding a perturbation term to the system of the pendulum (4) to represent friction, a physically more realistic situation. The motion of the pendulum bob obey the following equation

$$\begin{aligned} \theta' &= y, \\ y' &= -K \sin(\theta) - \epsilon y. \end{aligned} \quad (14)$$

where ϵ is a friction coefficient and we have assumed that the friction is proportional to the velocity. Substitute the Eq. (13) in the Eq. (14) to get the system

$$\begin{aligned} \theta' &= y, \\ y' &= -\frac{dV(\theta)}{d\theta} - \epsilon y. \end{aligned} \quad (15)$$

In particular, using the potential energy $V_\gamma(x) = \frac{x^2}{2} - \gamma \frac{x^3}{3} - \frac{x^4}{4}$, $\gamma > 0$ for the motion of the pendulum, $\epsilon = 0.1$, and replacing θ by x , we get the desired system

$$\begin{aligned} x' &= y, \\ y' &= -x + \gamma x^2 + x^3 - 0.1y. \end{aligned} \quad (16)$$

Figure 3 represents the potential $V_\alpha(x)$. It is clear that, the parameter α controls the difference in height of the two peaks and the x-coordinate of the two corresponding saddles. The blue curve is for $\alpha = 0.2$, black for $\alpha = 0.14$. and red for $\alpha = 0.1$. A heteroclinic bifurcation between the two saddles of the system (16) is detected in Sects. 3 and 4 at a value of α closed to 0.14.

This paper is organized as follows: In the next section, we study the stability of the equilibria of system (16). In Sect. 3, we study the bifurcations like heteroclinic saddle connections using numerical method through Maple software. The topological method is used in Sect. 4 to detect the heteroclinic bifurcation through the Conley index technique. In conclusion section, the results of the motion of pendulum are summarized, and future work is suggested.

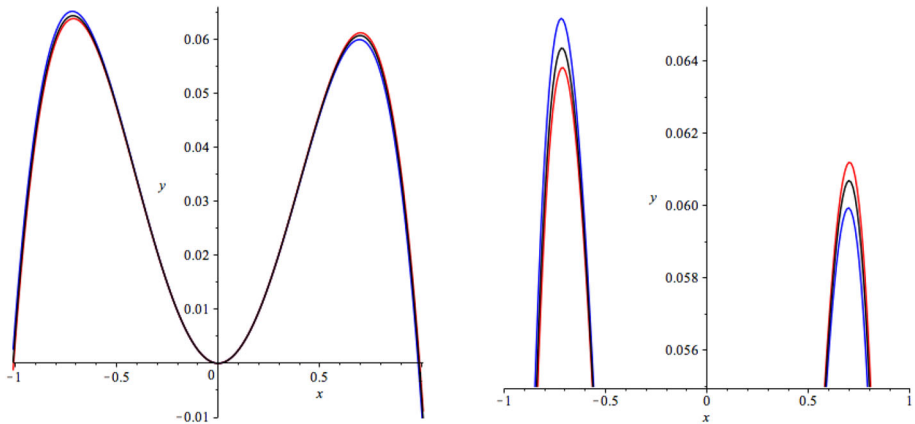


Fig. 3 Potential $V_\alpha(x)$ for the system (16)

Steady States and Their Stability

To study the stability of the equilibria of system (16), note that its Jacobian matrix takes the form

$$J = \begin{bmatrix} 0 & 1 \\ 3x^2 + 2\gamma x - 1 & -0.1 \end{bmatrix}. \tag{17}$$

The equilibria of system (16) are solutions of the equations

$$\begin{aligned} 0 &= y, \\ 0 &= -x + \gamma x^2 + x^3 - 0.1y. \end{aligned} \tag{18}$$

and are given by $E_0 = (0, 0)$, $E_1 = (A, 0)$ and $E_2 = (B, 0)$ where the values of A and B are determined in the Eqs. (19) and (20).

$$A = \frac{-\gamma + \sqrt{\gamma^2 + 4}}{2}, \quad \gamma > 0 \tag{19}$$

and

$$B = \frac{-\gamma - \sqrt{\gamma^2 + 4}}{2}, \quad \gamma > 0 \tag{20}$$

Since $\gamma > 0$, it follows that $A > 0$. We notice that when γ increases, the equilibrium point $(A, 0)$ moves from the point $(1, 0)$ toward the origin. In the same way, as we consider $\gamma > 0$, it follows that $B < 0$, and the equilibrium point $(B, 0)$ is moving away from the point $(-1, 0)$ to the left on the x -axis, see the graph of A and the graph of B in Fig. 4.

The Jacobian matrix evaluated at the equilibrium point $E_0 = (0, 0)$ is

$$J(E_0) = \begin{bmatrix} 0 & 1 \\ -1 & -0.1 \end{bmatrix}. \tag{21}$$

We summarize the stability of E_0 in the following theorem.

Theorem 2.1 *The equilibrium point $E_0 = (0, 0)$ is stable.*

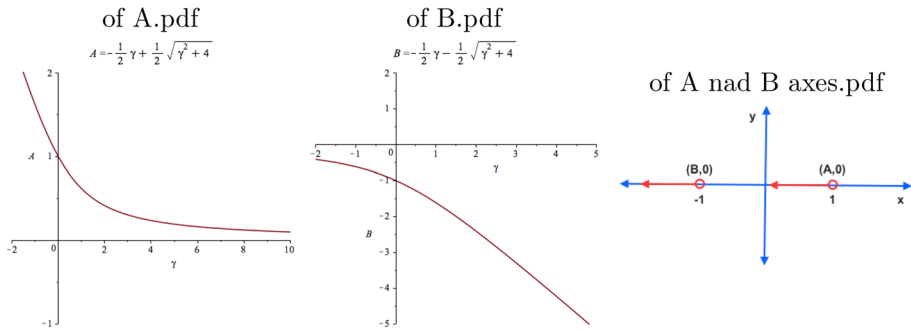


Fig. 4 Graph of A and graph of B

Proof From the Jacobian matrix (21), the eigenvalues of $J(E_0)$ are

$$\lambda_{1,2}|_{(0,0)} = \frac{-0.1 \pm i\sqrt{3.99}}{2}. \tag{22}$$

We notice that $Re(\lambda_{1,2}) < 0$ so E_0 is stable. □

We summarize the stability of $E_1 = (A, 0)$ and $E_1 = (B, 0)$ in the following theorem.

Theorem 2.2 *The equilibrium points $E_1 = (A, 0)$ and $E_1 = (B, 0)$ are saddles.*

Proof The Jacobian matrix evaluated at $E_1 = (A, 0)$ is

$$J(E_1) = \begin{bmatrix} 0 & 1 \\ 3A^2 + 2\gamma A - 1 & -0.1 \end{bmatrix}, \tag{23}$$

and so the eigenvalues of $J(E_1)$ are

$$\lambda_{1,2}|_{(A,0)} = \frac{-0.1 \pm \sqrt{-3.99 + 12A^2 + 8\gamma A}}{2}. \tag{24}$$

We notice from the Fig. 5 that $\lambda_1|_{(A,0)} = \frac{-0.1 + \sqrt{-3.99 + 12A^2 + 8\gamma A}}{2} > 0$ and $\lambda_2|_{(A,0)} = \frac{-0.1 - \sqrt{-3.99 + 12A^2 + 8\gamma A}}{2} < 0$, which means that E_1 is saddle. In the same way, we find that the eigenvalues of $J(E_2)$ are

$$\lambda_1|_{(B,0)} = \frac{-0.1 \pm \sqrt{-3.99 + 12B^2 + 8\gamma B}}{2}. \tag{25}$$

and hence, one eigenvalue is positive and the another one is negative, see Fig. 6 which means that E_2 is saddle. □

Numerical Approach

The heteroclinic bifurcation is a connection from α -limit set to ω -limit set, see [23]. Let Γ be a Hausdorff topological space with flow φ , then ω -limit set of a subset $Y \subset \Gamma$ is given by

$$\omega(Y) := \text{Inv}(\overline{\varphi(Y, [0, \infty))}) = \bigcap_{t>0} \overline{\varphi(Y, [t, \infty))}. \tag{26}$$

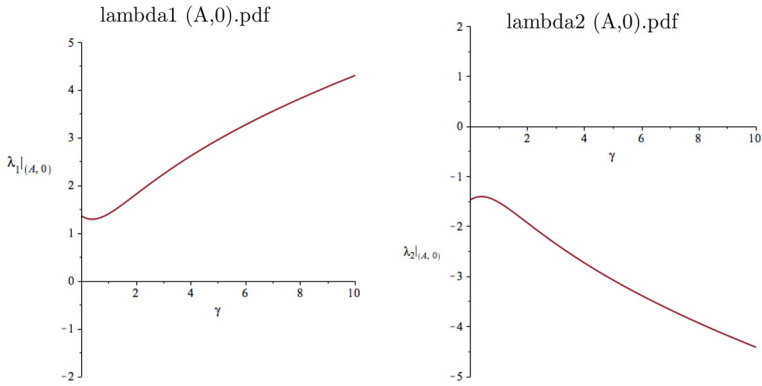


Fig. 5 Graph of eigenvalues at (A,0)

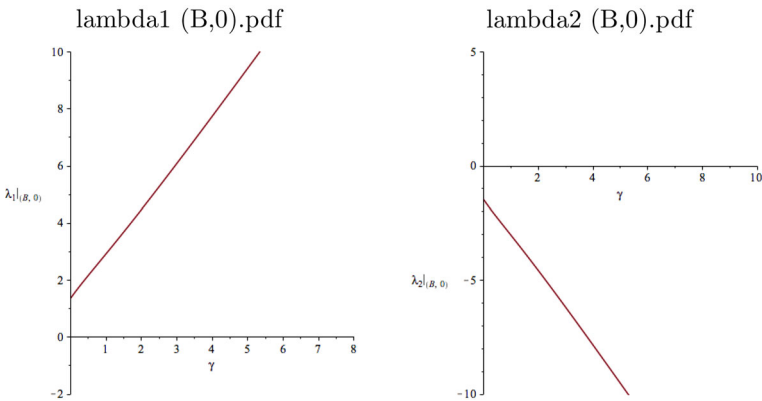


Fig. 6 Graph of eigenvalues at (B,0)

and the α -limit set (ω^* -limit set) of a subset $Y \subset \Gamma$ is given by

$$\alpha(Y) := \text{Inv}(\overline{\varphi(Y, (-\infty, 0])}) = \bigcap_{t < 0} \overline{\varphi(Y, (-\infty, t])}. \tag{27}$$

In this section, we study the numerical solution of the system (16), in particular we focus on three stages

1. Before the heteroclinic bifurcation, this case is explained in Table 1 and Fig. 7a in which we choose $\gamma \ll \gamma^*$.
2. After the heteroclinic bifurcation, this case is explained in Table 2 and Fig. 7b in which we choose $\gamma \gg \gamma^*$.
3. We approximate γ^* , which is the value of the parameter γ , where the heteroclinic bifurcation is happened. This case is explained in Table 3 and Fig. 7c.

The parameter γ controls the change of the solution structure in the dynamical system (16), and consequently the direction of the flow in its phase portrait is changing as the parameter γ is varying. We use the Maple software for screening the flow in the phase portrait as γ is growing. When $\gamma = 0.1$, the red trajectory that comes from the saddle $(B, 0)$ is underneath the blue trajectory that comes in the saddle $(A, 0)$ which is shown in Fig. 7a. In this situation,

Table 1 Before heteroclinic bifurcation

Initial point	Time	Color
(−1.05066846703369, 0.000814079843825949)	$t = 0 \dots 30$	Red
(−1.05182997296631, −0.000814079843825949)	$t = 0 \dots 5$	Teal
(−1.05180346832364, 0.000832351365552794)	$t = -5 \dots 0$	Green
(−1.05069497167636, −0.000832351365552794)	$t = -8 \dots 0$	Brown
(0.951849870183757, 0.000799511949099649)	$t = 0 \dots 5$	Orange
(0.950648569816243, −0.000799511949099649)	$t = 0 \dots 30$	Magenta
(0.950676432222895, 0.000819703704029008)	$t = -9 \dots 0$	Blue
(0.951822007777105, −0.000819703704029008)	$t = -5 \dots 0$	Yellow

Table 2 After heteroclinic bifurcation

Initial point	Time	Color
(−1.10441747062513, 0.000821581295001963)	$t = 0 \dots 10$	Red
(−1.10555765337487, −0.000821581295001963)	$t = 0 \dots 5$	Teal
(−1.10553188406442, 0.000838876325919179)	$t = -5 \dots 0$	Green
(−1.10444323993558, −0.000838876325919179)	$t = -8 \dots 0$	Brown
(0.905597381649791, 0.000792540216473987)	$t = 0 \dots 5$	Orange
(0.904377742350209, −0.000792540216473987)	$t = 0 \dots 30$	Magenta
(0.904406222213875, 0.000813660895624604)	$t = -12 \dots 0$	Blue
(0.905568901786125, −0.000813660895624604)	$t = -5 \dots 0$	Yellow

Table 3 At heteroclinic bifurcation

Initial point	Time	Color
(−1.07261973731311, 0.000817172852276827)	$t = -2 \dots 30$	Red
(−1.07377252268689, −0.000817172852276827)	$t = 0 \dots 5$	Teal
(−1.07374631822994, 0.000835040664658527)	$t = -5 \dots 0$	Green
(−1.07264594177006, −0.000835040664658527)	$t = -8 \dots 0$	Brown
(0.932400641744550, 0.000796596228148902)	$t = 0 \dots 5$	Orange
(0.931191618255450, −0.000796596228148902)	$t = 0 \dots 30$	Magenta
(0.931219741418219, 0.000817175747799663)	$t = -11 \dots 0$	Blue
(0.932372518581781, −0.000817175747799663)	$t = -5 \dots 0$	Yellow

it is clear that the saddle $(B, 0)$ is α -limit set which plays as a repeller and the saddle $(A, 0)$ is ω -limit set which plays as a attractor. We can find the initial points of the colored trajectories of the solution in the Table 1. This case is known as “before heteroclinic bifurcation” which is mentioned in stage 1. In the second stage, we notice that when $\gamma = 0.2$ the red trajectory changes its position to become above the blue trajectory. This case is shown in Fig. 7b, and its initial points of the colored trajectories of the solution are illustrated in the Table 2, and it is known as “after heteroclinic bifurcation” which is pointed to in stage 2. The heteroclinic bifurcation is detected at $\gamma = \gamma^* \approx 0.1414$ where the red and blue trajectories are merged. This case is happened when γ increases, the red trajectory moves upward and the blue

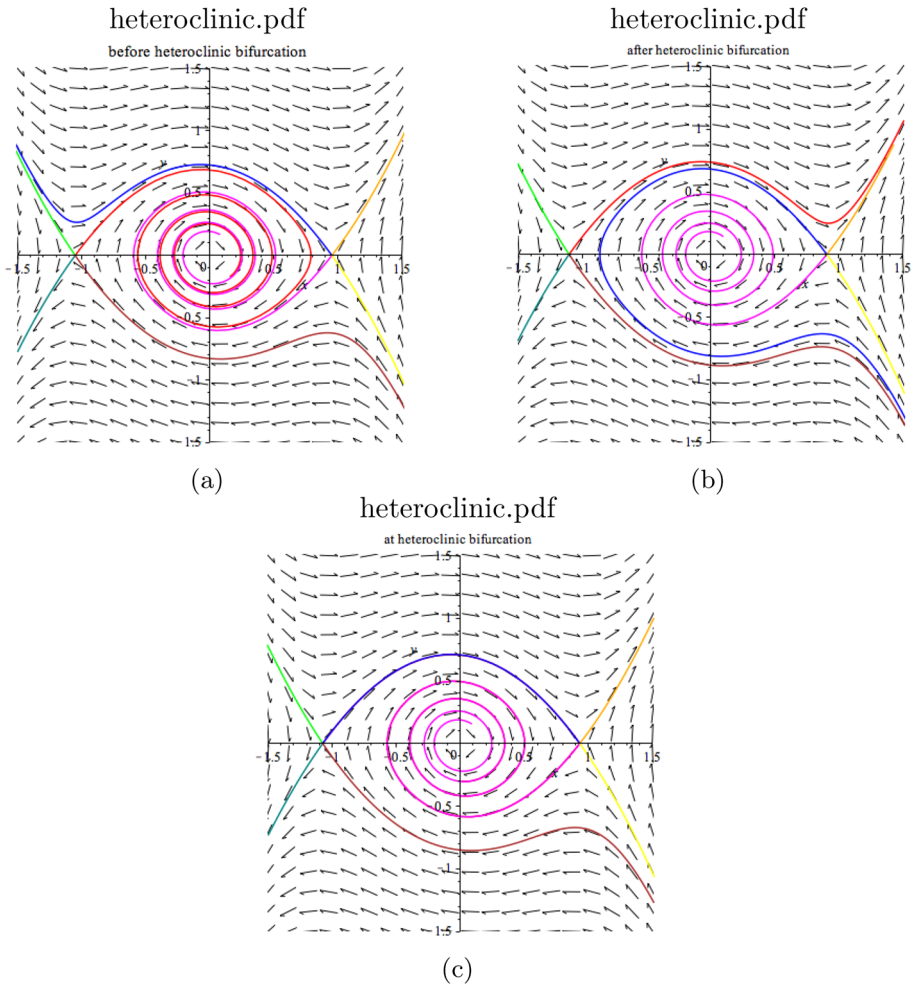


Fig. 7 a Before, b after and c at heteroclinic bifurcation

trajectory moves downward and they are consolidated at the value γ^* . This bifurcation is shown in Fig. 7c, and the initial points of the colored trajectories of the solution for this stage are explained in the Table 3. This kind of bifurcation is called “heteroclinic bifurcation” which is mentioned in stage 3.

Topological Method

To investigate the existence and behavior of a system’s families of solutions, topological techniques can be combined with rigorous numerical computation. At any parameter value, the dynamical system can be represented by a Conley–Morse graph which is a directed graph with certain algebraic information (Homology groups). Changes of dynamics (at different parameter values) can be registered by changes in the Conley–Morse graphs.

Table 4 Conley index of some basic isolated invariant sets

If p is a sink (stable)	$CH_q(p) = \mathbb{Z}_2$ if $q = 0$
If p is a saddle in the plane	$CH_q(p) = \mathbb{Z}_2$ if $q = 1$

In this section we state necessary definitions and theorems to detect the heteroclinic saddle connection, for more information see [5, 9–11, 21, 25, 27]. We use homology with coefficients in the finite field \mathbb{Z}_2 , S will always denote an isolated invariant set and the homological Conley index of S , $CH_q(S)$, is the relative homology $H_q(N, L)$, where q is a homology index.

Definition 4.1 A pair of compact sets (N, L) is called an index pair of S where $L \subset N \subset \mathbb{R}^n$ if

1. $S = \text{Inv}(\overline{N \setminus L})$, and $\overline{N \setminus L}$ is an isolating neighborhood of S in X ,
2. L is positively invariant in N that is given $x \in L$ and $\varphi(x, [0, t]) \subset N$, then $\varphi(x, [0, t]) \subset L$,
3. L is an exit set for N that is given $x \in N$ and $t_1 > 0$ such that $\varphi(x, t_1) \notin N$, then there exists $t_0 \in [0, t_1]$ such that $\varphi(x, [0, t_0]) \subset N$ and $\varphi(x, t_0) \in L$.

The homotopical Conley index of S , $h(S)$, is defined as the pointed homotopy type of the quotient space N/L . We summarize the Conley index of some basic isolated invariant sets in Table 4.

A *partial order* on a set \mathcal{P} is a relation $<$ on \mathcal{P} that satisfies: if (1) $\pi < \pi'$ never holds for $\pi \in \mathcal{P}$, and (2) if $\pi < \pi'$ and $\pi' < \pi''$ then $\pi < \pi''$.

Definition 4.2 Let $(\mathcal{P}, <)$ be a partially ordered set. A subset $I \subset \mathcal{P}$ is called an *interval* if $p < r < q$ with $p, q \in I$ implies $r \in I$. The set of intervals in $<$ is denoted $I(<)$. Points $p, q \in \mathcal{P}$ are called *adjacent* if $\{p, q\} \in I(<)$, i.e., $\{p, q\}$ or $\{q, p\}$ is an interval in \mathcal{P} .

If $p, q \in \mathcal{P}$ and neither $p < q$ nor $q < p$, then we say that p and q are noncomparable.

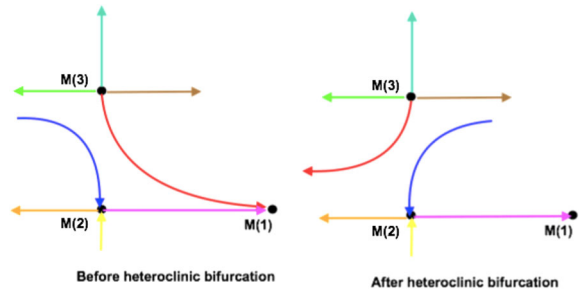
Definition 4.3 Let S be a compact invariant set (not necessarily isolated). A $(<-)$ -ordered *Morse decomposition* of S is a collection $M(S) = \{M(p) \mid p \in \mathcal{P}\}$ of mutually disjoint compact invariant subsets of S such that if $x \in S \setminus \bigcup_{p \in \mathcal{P}} M(p)$, then there exist $q < p$ ($p, q \in \mathcal{P}$) with $\omega(x) \subset M(q)$ and $\alpha(x) \subset M(p)$, i.e., $x \in C(M(p), M(q))$ (connection from $M(p)$ to $M(q)$).

In general, any ordering on \mathcal{P} satisfying the above property is called admissible (for the flow). The invariant set $M(p)$ is called Morse set. Moreover, if S is isolated, then each $M(p)$ is also isolated. The flow on S defines an ordering on Morse sets and, hence a partial order $<_F$ on \mathcal{P} . $<_F$ is defined by setting $\pi' <_F \pi$ if and only if there exists a sequence of distinct elements of \mathcal{P} , $\pi' = \pi_0, \dots, \pi_n = \pi$, such that $C(\pi_j, \pi_{j-1}) \neq \emptyset$ for each $j = 1, \dots, n$. A subset $A \subset S$ is an attractor in S if there exists an open neighborhood U of A in S such that $A = \omega(U)$. If A is an attractor in S , the dual repeller of A in S is defined by $A^* := \{x \in S \mid \omega(x) \cap A = \emptyset\}$. In the flow ordering on invariant subsets of S , we write $A <_F A^*$ to indicate that a flow comes from the repeller A^* and lands at the attractor A .

Definition 4.4 Let S be an isolated invariant set (in a local flow X), and let the collection of invariant sets $\{M(p) \mid p \in (\mathcal{P}, <)\}$ be a Morse decomposition of S with admissible ordering $<$, then an associated connection matrix is a linear map

$$\Delta : \bigoplus_{p \in \mathcal{P}} CH_*(M(p)) \rightarrow \bigoplus_{p \in \mathcal{P}} CH_*(M(p)),$$

Fig. 8 Conley–Morse graph of the flow before and after the bifurcation



where $\Delta(p, q) : CH_*(M(q)) \rightarrow CH_*(M(p))$ is the corresponding (p, q) -component of Δ such that the following conditions are satisfied:

1. Δ is strictly upper triangular, so that if $\Delta(p, q) \neq 0$ implies $p < q$.
2. Δ is a boundary map if each $\Delta(p, q)$ is of degree -1 and $\Delta^2 = 0$.
3. For every interval I , $CH_*(M(I)) \cong \frac{Ker \Delta(I)}{Im \Delta(I)}$.

The collection of all connection matrices of a system with a parameter γ is denoted by $\mathcal{C}\mathcal{M}(M_\gamma)$, where γ is defined on some open interval.

Let (X, d) be a compact metric space, and Λ be an interval in \mathbb{R} . Then a parametrized family of local flows is

$$\phi : (X \times \Lambda) \times \mathbb{R} \rightarrow X$$

such that $\phi^\lambda | X^\lambda = \phi | X \times \{\lambda\}$ is a local flow for each $\lambda \in \Lambda$.

There is a space of isolated invariant sets for the product parameterization with underlying set

$$\mathcal{S} = \mathcal{S}(\phi) = \{(S^\lambda, X^\lambda) | S^\lambda \text{ is an isolated invariant set in } X^\lambda\}.$$

Theorem 4.5 [5] *If S^λ and S^μ are related by continuation and c is a path in \mathcal{S} from S^λ to S^μ then (associated to the path-homotopy class of c) there is a homotopy equivalence $\theta_{[c]} : h(S^\lambda) \rightarrow h(S^\mu)$.*

The homotopy equivalence $\theta_{[c]}$ induces a homology isomorphism $CH_*(S^\lambda) \rightarrow CH_*(S^\mu)$.

Corollary 4.6 [10, Corollary 5.2] *If c is as in Theorem 4.5, then there is an isomorphism $(\theta_{[c]})_* : CH_*(S^\lambda) \rightarrow CH_*(S^\mu)$ associated to the path homotopy class of c .*

The most important property of the connection matrices is stated in the following theorem

Theorem 4.7 [11] *If $\Delta \in \mathcal{C}\mathcal{M}(M)$, p and q are adjacent in the flow ordering, and $\Delta(p, q) \neq 0$, then $C(M(q), M(p)) \neq \emptyset$.*

Back to the system (16), the flow of the Fig. 7 can be depicted as in Fig. 8 where the Conley–Morse graph is used to study the changes of dynamics when the parameter $\gamma \ll \gamma^*$ and $\gamma \gg \gamma^*$.

The Morse sets: $M(1)$ represents the stable equilibrium $(0, 0)$, $M(2)$ represents the saddle equilibrium point $(A, 0)$ and $M(3)$ represents the saddle equilibrium point $(B, 0)$.

We use the connection matrix continuation theory to prove that there exists a parameter value γ^* such that $C(M_{\gamma^*}(3), M_{\gamma^*}(2)) \neq \emptyset$. We start studying the system (16) when the parameter varies in the interval $\gamma \in (0, \gamma^*)$, and we observe over this interval that there are two orbits from the saddles to the sink. Therefore, if $0 < \gamma \ll \gamma^*$, then $\mathcal{C}\mathcal{M}(M_\gamma)$ contains

a single matrix, and it is in the form Δ_1 with admissible ordering $<_1$. To find the connection matrix Δ_1 , let S_1 be the compact invariant set of the graph “Before heteroclinic bifurcation” in Fig. 8, then S_1 consists of the Morse sets $\{M(1), M(2), M(3)\}$ and the connections $\{C(M(2), M(1)), C(M(3), M(1))\}$. Then a $(<_1$ -ordered) Morse decomposition of S_1 is a collection $M(S_1) = \{M(p) \mid p \in \mathcal{P}_1 = \{1, 2, 3\}\}$ with flow ordering $M(1) <_1 M(2)$ and $M(1) <_1 M(3)$. Then

$$\Delta_1 = \begin{matrix} & H_0(1) & H_1(2) & H_1(3) \\ \begin{matrix} H_0(1) \\ H_1(2) \\ H_1(3) \end{matrix} & \begin{pmatrix} 0 & \cong & \cong \\ 0 & 0 & 0 \\ 0 & 0 & 0 \end{pmatrix} \end{matrix}. \tag{28}$$

In the matrix Δ_1 , we use the letter H to represent the homological Conley index such that $H_0(1)$ represents the Morse set $M(1)$ with its Conley index $q = 0$, $H_1(2)$ represents the Morse set $M(2)$ with its Conley index $q = 1$, and $H_1(3)$ represents the Morse set $M(3)$ with its Conley index $q = 1$. For example the entry $\Delta_1(1, 3)$ represents $(H_0(1), H_1(3))$. We put $\Delta_1(1, 2) = \cong$ to indicate that there is a connection orbit from $H_1(2)$ to $H_0(1)$, the same way for $\Delta_1(1, 3) = \cong$. Also from the definition 4.4, the matrix Δ_1 is strictly upper triangular, and each entry in Δ_1 has degree -1 , we must have $\Delta_1(2, 3) = 0$ ($H_1(2)$ and $H_1(3)$ are saddles so their indices are equal, see Table 4, so the degree from $H_1(3)$ to $H_1(2)$ is not -1 , and hence $\Delta_1(2, 3) = 0$, see condition two in Definition 4.4).

If $\gamma >> \gamma^*$, we notice that $H_1(3)$ and $H_0(1)$ are noncomparable under the flow ordering, then $\mathcal{C.M}(M_\gamma)$ contains a single matrix, and it is in the form Δ_2 in which $\Delta_2(1, 3) = 0$. In the same technique, let S_2 be the compact invariant set of the graph “After heteroclinic bifurcation” in Fig. 8, then a $(<_2$ -ordered) Morse decomposition of S_2 is a collection $M(S_2) = \{M(p) \mid p \in \mathcal{P}_2 = \{1, 2, 3\}\}$ with flow ordering $M(1) <_2 M(2)$. Then

$$\Delta_2 = \begin{matrix} & H_0(1) & H_1(2) & H_1(3) \\ \begin{matrix} H_0(1) \\ H_1(2) \\ H_1(3) \end{matrix} & \begin{pmatrix} 0 & \cong & 0 \\ 0 & 0 & 0 \\ 0 & 0 & 0 \end{pmatrix} \end{matrix}.$$

From the Conley–Morse graphs and admissible partial orderings of the Morse sets of the “Before heteroclinic bifurcation” and “After heteroclinic bifurcation” Morse decomposition, one can compute in each case a unique connection matrix. Let $\mathcal{C.M}_1$ and $\mathcal{C.M}_2$ be the first and the second collections of connection matrices respectively represented above. Define $\gamma_i \in \{\gamma \in (0, \infty) \mid \mathcal{C.M}(M_\gamma) = \mathcal{C.M}_i\}$ for $i = 1, 2$. We notice that γ_1 and γ_2 are disjoint and both nonempty. The local connection matrix continuation theorem in [10] and the connection matrix existence theorem in [11] imply that each γ_i is open. The connection matrix continuation theory says that there exists a parameter $\gamma^* \in (0, \infty) \setminus \{\gamma_1 \cup \gamma_2\}$ where the set of connection matrices $\mathcal{C.M}(M_{\gamma^*})$ contains both matrices

$$\begin{pmatrix} 0 & \cong & \cong \\ 0 & 0 & 0 \\ 0 & 0 & 0 \end{pmatrix} \text{ and } \begin{pmatrix} 0 & \cong & 0 \\ 0 & 0 & 0 \\ 0 & 0 & 0 \end{pmatrix}. \tag{29}$$

$\Delta(1, 3)$ is nontrivial in the first matrix, therefore $1 <_F 3$ in the flow ordering of M_{γ^*} . We claim that $M_{\gamma^*}(1)$ and $M_{\gamma^*}(3)$ are not adjacent under the flow ordering. Suppose they are adjacent, then according to the computations of γ_1 and γ_2 , the $\Delta(1, 3)$ connection matrix entry is uniquely determined and is either an isomorphism or trivial (I.e., 0 or \cong). However, $\Delta(1, 3)$ is not uniquely determined, and this proves the claim. This implies that $1 <_F 2 <_F 3$, then $C(M_{\gamma^*}(3), M_{\gamma^*}(2)) \neq \emptyset$. Therefore, there is a connecting orbit at γ^* between the saddles

Table 5 Comparison of some investigation methods for the heteroclinic bifurcation in the pendulum

Author	Method
Dabbs and Smith	Planar Melnikov techniques
Elnaggar and Elkobrsy	Melnikov functions
Kevrekidis and others	Discretization of spatial or temporal derivatives
Huafeng and Jianshe	The variational method and delicate analysis technique

$M_{\gamma^*}(2)$ and $M_{\gamma^*}(3)$ which is the heteroclinic bifurcation in the motion of pendulum that is described in the system (16).

The heteroclinic bifurcation was investigated in many methods for many formulas of pendulum equations, we can summarize some of these methods in the Table 5.

Conclusion

A motion of the pendulum is represented by a system of first ODE, and it has an interesting heteroclinic bifurcation, this bifurcation is detected by numerical-topological method. Combining the rigorous numerical computation to the topological method confirm the existence of the heteroclinic bifurcation in the system (16). In future work, we suggest improving the system (16) of the pendulum by modifying the friction term to detect a homoclinic bifurcation using numerical-topological method.

Acknowledgements The authors would like to thank the referees for the helpful suggestions to improve the paper.

Author Contributions All authors read and approved the final manuscript.

Funding No funding.

Availability of Data and Materials Data sharing not applicable to this article as no data sets were generated or analyzed during the current study.

Declarations

Conflict of interest The authors declare that they have no competing interests.

Consent for Publication Not applicable

References

1. Abdulkareem, S., Akgül, A., Jalal, V., Faraj, B., Abdullah, O.: Numerical solution for time period of simple pendulum with large angle. *Therm. Sci.* **24**, 09 (2020)
2. Baleanu, D., Hassan Abadi, M., Jajarmi, A., Zarghami Vahid, K., Nieto, J.J.: A new comparative study on the general fractional model of covid-19 with isolation and quarantine effects. *Alex. Eng. J.* **61**(6), 4779–4791 (2022)
3. Big-Alabo, A., Ossia, C.V.: Periodic oscillation and bifurcation analysis of pendulum with spinning support using a modified continuous piecewise linearization method. *Int. J. Appl. Comput. Math.* **5**(4), 16 (2019)

4. Chessin, A.S.: On Foucault's pendulum. *Am. J. Math.* **17**(1), 81–88 (1895)
5. Conley, C.: *Isolated Invariant Sets and the Morse Index*. CBMS Regional Conference Series in Mathematics, vol. 38. American Mathematical Society, Providence, RI (1978)
6. Dabbs, M.F., Smith, P.: Critical forcing for homoclinic and heteroclinic orbits of a rotating pendulum. *J. Sound Vib.* **189**(2), 231–248 (1996)
7. Elnaggar, F.A., Elkobry, G.A.: Homoclinic and heteroclinic bifurcations of the motion of rotating pendulum. *Proc. Annu. Southeast. Symp. Syst. Theor.* **36**, 338–343 (2004)
8. Erturk, V.S., Godwe, E., Baleanu, D., Kumar, P., Asad, J., Jajarmi, A.: Novel fractional-order Lagrangian to describe motion of beam on nanowire. *Acta Phys. Polon. A* **140**(3), 265–272 (2021)
9. Franzosa, R.: Index filtrations and the homology index braid for partially ordered Morse decompositions. *Trans. Am. Math. Soc.* **298**(1), 193–213 (1986)
10. Franzosa, R.D.: The continuation theory for Morse decompositions and connection matrices. *Trans. Am. Math. Soc.* **310**(2), 781–803 (1988)
11. Franzosa, R.D.: The connection matrix theory for Morse decompositions. *Trans. Am. Math. Soc.* **311**(2), 561–592 (1989)
12. Gaul, M., Kuczmariski, F.: Not-so-simple pendulums. *Math. Mag.* **94**(1), 3–15 (2021)
13. Han, N., Cao, Q.: Global bifurcations of a rotating pendulum with irrational nonlinearity. *Commun. Nonlinear Sci. Numer. Simul.* **36**, 431–445 (2016)
14. Hubbard, J.H., West, B.H.: *Differential Equations: A Dynamical Systems Approach*. Texts in Applied Mathematics, vol. 18. Springer, New York (1995)
15. Hughes, J.V.: Possible motions of a sphere suspended on a string (the simple pendulum). *Am. J. Phys.* **21**, 47–50 (1953)
16. Amin Jajarmi, D., Baleanu, D., Zarghami Vahid, K., Mohammadi Pirouz, H., Asad, J.: A new and general fractional Lagrangian approach: a capacitor microphone case study. *Results Phys.* **31**, 104950 (2021)
17. Jajarmi, A., Baleanu, D., Vahid, K.Z., Mobayen, S.: A general fractional formulation and tracking control for immunogenic tumor dynamics. *Math. Methods Appl. Sci.* **45**(2), 667–680 (2022)
18. Kevrekidis, P.G., Jones, C.K.R.T., Kapitula, T.: Exponentially small splitting of heteroclinic orbits: from the rapidly forced pendulum to discrete solitons. *Phys. Lett. A* **269**(2–3), 120–129 (2000)
19. Lampret, V.: How is the period of a simple pendulum growing with increasing amplitude? *Math. Slov.* **71**(2), 359–368 (2021)
20. Loveikin, V.S., Romasevich, Y.A., Khoroshun, A.S., Shevchuk, A.G.: Time-optimal control of a simple pendulum with a movable pivot. Part 2. *Int. Appl. Mech.* **56**(2), 208–215 (2020) (**Translation of Prikl. Mekh.** **56**(2), 95–103 (2020))
21. Mischaikow, K.: Existence of generalized homoclinic orbits for one parameter families of flows. *Proc. Am. Math. Soc.* **103**(1), 59–68 (1988)
22. Neishtadt, A.I., Sheng, K.: Bifurcations of phase portraits of pendulum with vibrating suspension point. *Commun. Nonlinear Sci. Numer. Simul.* **47**, 71–80 (2017)
23. Perko, L.: *Differential Equations and Dynamical Systems*, volume 7 of Texts in Applied Mathematics, 3rd edn. Springer, New York (2001)
24. Rabinowitz, P.H.: Periodic and heteroclinic orbits for a periodic Hamiltonian system. *Ann. Inst. H. Poincaré Anal. Non Linéaire* **6**(5), 331–346 (1989)
25. Reineck, J.F.: Connecting orbits in one-parameter families of flows. *Ergod. Theory Dyn. Syst.* **8**(Charles Conley Memorial Issue), 359–374 (1988)
26. Sakthivel, G., Rajasekar, S.: Diffusion dynamics near critical bifurcations in a nonlinearly damped pendulum system. *Commun. Nonlinear Sci. Numer. Simul.* **17**(3), 1301–1311 (2012)
27. Salamon, D.: Connected simple systems and the Conley index of isolated invariant sets. *Trans. Am. Math. Soc.* **291**(1), 1–41 (1985)
28. Sharma, A., Patidar, V., Purohit, G.: Bifurcation and chaos in periodically forced and nonlinearly damped pendulum. *Int. J. Nonlinear Sci. Numer. Simul.* **14**(3–4), 179–188 (2013)
29. Xiao, H., Jianshe, Yu.: Heteroclinic orbits for a discrete pendulum equation. *J. Differ. Equ. Appl.* **17**(9), 1267–1280 (2011)
30. Zhou, L., Liu, S., Chen, F.: Subharmonic bifurcations and chaotic motions for a class of inverted pendulum system. *Chaos Solitons Fractals* **99**, 270–277 (2017)